Analysis-Synthesis of Saxophone Input Impedances via Recursive Parallel Filters

Esteban Maestre,[1†] *Julius O. Smith,*[2] *Gary P. Scavone*[1]

[1]Computational Acoustic Modeling Laboratory, McGill University
[2]Center for Computer Research in Music and Acoustics, Stanford University
[†]esteban@music.mcgill.ca

ABSTRACT

We introduce an analysis-synthesis framework for simulation of wind instrument input impedances as recursive digital filters in parallel form, derived from measured data. For analysis, we iteratively minimize the error between the frequency response of a saxophone input impedance measurement and that of a synthetic impedance model constructed from a digital filter structure akin to the discretization of a modal expansion. The input impedance model is used to derive a reflectance filter and used for efficient sound synthesis via a reed model based on non-linear scattering.

1. INTRODUCTION

As efficient sound synthesis schemes, most digital waveguide models [1] of wind instruments approximate their air columns as being cylindrical. In a typical digital waveguide model, the air column of an ideal instrument constructed from a cylindrical pipe and a bell can be represented by a pair of delay lines simulating pressure wave propagation inside the pipe, and a termination that includes two digital filters: one that lumps frequency-dependent propagation losses and dispersion, and another one emulating the frequency-dependent bell reflectance. In these efficient schemes, the reed-valve end termination of the pipe is often modeled via a non-linear scattering element that is interfaced to the air column model through decomposed pressure traveling waves P^+ and P^-, respectively going into and reflected back from the pipe input interface. Approximations with conical elements are possible but often result in inharmonic resonance structures that are difficult to tune for sound synthesis.

To account for realistic, non-ideal instrument air column shapes, one could treat the entire air column as a resonant load, observe its linear behavior from frequency-domain experimental data, and design an *air column load* impedance filter model $Z(z)$ (i.e., an input impedance filter) for simulation so that the reflected pressure wave $P^-(z)$ can be obtained from the incident wave $P^+(z)$ via $P^-(z) = R(z)P^+(z)$, with $R(z)$ being a digital reflectance model derived from $Z(z)$. In a previous work [2], a frequency-domain measurement of an air column input impedance is used to construct a discrete time reflection function $r[n]$ that is suitable for a traveling wave numerical scheme based on convolution. Authors propose a method to evade the time-aliasing and other numerical problems that naturally arise from estimating $r[n]$ via inverse Fourier transform of a frequency-domain measurement signal.

The motivation of this work lies in avoiding the aforementioned problems by proposing a methodology for translating input impedance measurements directly into recursive digital filters of moderately low order, with the added advantage that efficiency is improved with respect to discrete convolution. We construct a digital model $Z(z)$ of the air column input impedance by means of recursive digital filters in parallel form, so that a corresponding digital reflectance $R(z)$ can be connected to a reed-valve non-linear scattering model under the traveling wave formulation. Although applicable to other wind instruments, the design of such impedance filter is carried out here by fitting its coefficients to a measured saxophone input impedance obtained from experimental data.

Alto saxophone input impedances were measured using a six-microphone probe, calibrated with three non-resonant loads, via a least-mean square signal processing technique as described in [3]. In Figure 1 we display the magnitude of an alto saxophone input impedance measurement (grey curve), obtained for a 'Bb3' fingering, and normalized to the characteristic wave impedance of the air column input. As the resonance amplitudes decrease with frequency, the normalized impedance tends to a value of 1, i.e., total transmission.

2. THE INPUT IMPEDANCE AS A RECURSIVE PARALLEL FILTER

By attending to the resonance structure of input impedance measurements, it appears clear that we can benefit from proposing a digital filter formulation that is akin to the discretization of a modal expansion. In fact, in a previous paper we addressed a similar problem for the case of bridge input admittances in string instruments [4]. Here we construct an input impedance digital model $Z(z)$ by creating a digital modal basis over which impedance measurements are projected. Each m-th impedance modal basis function $H_m(z)$ is defined as

$$H_m(z) = \frac{1 - z^{-1}}{(1 - p_m z^{-1})(1 - p_m^* z^{-1})}, \qquad (1)$$

which corresponds to a two-pole resonator with one added zero at DC. The resonator is defined by a pair of complex conjugate poles p_m and p_m^*, which we relate to the corresponding modal frequency f_m and bandwidth β_m by $2\pi f_m / f_s = \angle p_m$ and $\beta_m = -\log|p_m|/\pi$, with f_s being the sampling frequency in Hertz. The impedance model $Z(z)$ is formulated in parallel as

$$Z(z) = \sum_{m=1}^{M} (r_{0,m} + r_{1,m} z^{-1}) H_m(z), \qquad (2)$$

where $r_{0,m}$ and $r_{1,m}$ are real-valued coefficients that allow control of both the amplitude and the phase of the the m-th resonator. The main reason behind the choice for our parallel resonator structure is that, while enabling the control of the relative phase between resonators, it imposes a gain of zero at DC irrespective of the coefficients $r_{0,m}$ and $r_{1,m}$.

3. IMPEDANCE FILTER DESIGN

Departing from a frequency-domain measurement of the target impedance $\hat{Z}$, the problem of designing the coefficients of a recursive digital filter model (2) that approximates the measurement can be stated as the minimization of an error measurement $\varepsilon(Z, \hat{Z})$ between the measurement and the model, with parameters being a vector $\boldsymbol{p} = \{p_1, \cdots, \omega_M\}$ of complex poles each corresponding the m-th resonator of of the model, and vectors $\mathbf{r}_0 = \{r_{0,1}, \cdots, r_{0,M}\}$ and $\mathbf{r}_1 = \{r_{1,1}, \cdots, r_{1,M}\}$ of respective numerator coefficients. We solve this problem via sequential quadratic programming [5]. At each iteration only pole positions are exposed as the variables to optimize: once they are decided, zeros (i.e., numerator coefficients) are constrained to minimize an auxiliary quadratic cost function, resulting in a simple closed-form solution. The positions of the poles are optimized iteratively: at each step, an error function is successively evaluated by projecting the target frequency response over a basis of frequency responses defined by the pole positions under test. We add a set of linear constraints to guarantee feasibilty and to ease convergence. This optimization routine is devised as an extension to the digital filter design technique proposed in [6].

3.1. Impedance measurement pre-processing

As it can be observed in the grey curves of Figure 1, the high-frequency region of an impedance measurement tipycally presents artifacts caused by noise and limitations of the measurement method. It is important to remove those artifacts so that the target normalized impedance effectively tends to 1 as frequency increases. This is needed to help the fitting process in providing an impedance model design for which the normalized impedance also tends to 1 in the high frequency region; otherwise, a derived air column reflectance filter would deliver reflected pressure waves with significant energy around Nyquist, and therefore cause undersired behaviors in the reed-valve non-linear scattering model. To this end, we perform cross-fading between the normalized impedance measurement and a constant value of 1, as illustrated in Figure 1, where we display the magnitude response of a pre-processed measurement.

3.2. Initialization and problem statement

We initialize the model parameters via finding a set of initial pole positions by attending to the magnitude response of the impedance measurement. First, resonance peak selection in the low-frequency region is carried out through an automatic procedure that iteratively rates and sorts spectral peaks by attending to a salience descriptor. For estimating modal frequencies, three magnitude samples (respectively corresponding to the corresponding maximum and its adjacent samples) are used to perform parabolic interpolation around selected peaks. For estimating bandwidths, the *half-power* rule [1] is applied using a linear approximation. For the high-frequency region we spread an additional set of poles, uniformly distributed on a logarithmic frequency axis. This leads to a total M modes, each expressed in terms of complex pole angles and radiae in the z-plane.

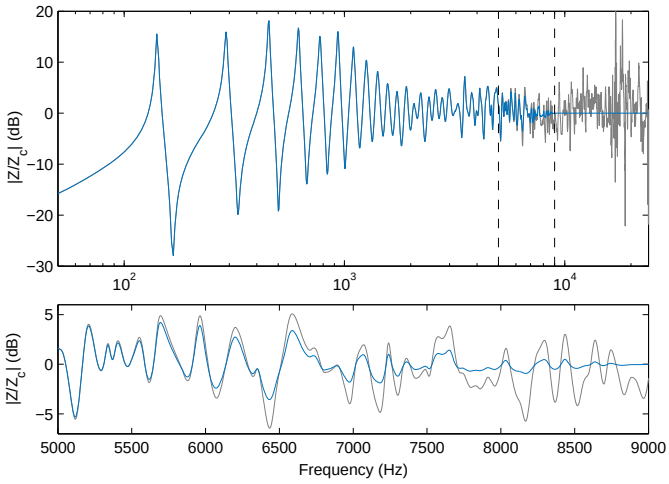

Figure 1. Magnitude response of an alto saxophone impedance measurement ('Bb3' fingering), normalized by the characteristic impedance of the input of the air column. Grey and blue curves are respectively used for raw and pre-processed data. Top: full band, with cross-fading region delimited by vertical lines. Bottom: cross-fading region.

We parametrize the initial set of M modes by representing each respective m-th complex pole pair in terms of its angle parameter $w_m = |\angle p_m|$ and its radius parameter $s_m = -\log(1 - |p_m|)$. This leads to two parameter sets: a set $\boldsymbol{w} = \{w_1 \cdots w_M\}$ of angle parameter values, and a set $\mathbf{s} = \{s_1 \cdots s_M\}$ of radius parameter values. With the new parametrization, we state the problem as

$$\begin{aligned} \underset{\boldsymbol{w},\mathbf{s}}{\text{minimize}} \quad & \varepsilon(Z, \hat{Z}) \\ \text{subject to} \quad & \mathbf{C}, \end{aligned} \tag{3}$$

where $\mathbf{C}$ is a set of linear constraints, and numerator coefficients have been left out as they are not exposed as variables in the optimization.

A key step before contraint definition is to sort the pole parameter sets so that linear constraints can be defined in a straightforward manner to ensure that the arrangement of poles in the unit disk is preserved during optimization, therefore reducing the number of crossings over local minima. Elements in sets $\mathbf{w}$ and $\mathbf{s}$ are jointly sorted as pairs (each pair corresponding to a complex-conjugate pole) by ascending angle parameter w_m.

3.3. Constraint definition

From ordered sets $\boldsymbol{w}$ and $\mathbf{s}$, linear onstraints $\mathbf{C}$ are defined as follows. First, feasibility is ensured by $0 \leq s_m$ and $0 \leq w_m \leq \pi$. Second, to aid convergence we constrain the pole sequence order in set $\boldsymbol{w}$ to be respected. This is expressed by $w_{m-1} < w_m < w_{m+1}$. Moreover, assuming that initialization provides an already trusted first solution, we can bound the search to a region around the initial pole positions. This can be expressed via the additional inequalities $w_m^- < w_m < w_m^+$ and $s_m^- < s_m < s_m^+$, where '$-$' and '$+$' superscripts are used to respectively indicate lower and upper bounds.

3.4. Error computation

At each i-th step of the optimization, the error $\varepsilon(Z, \hat{Z})$ is measured as follows. Given K samples of the target impedance frequency response $\hat{Z}(\omega)$ and the set $\mathbf{p}$ of M complex poles defining the modes at the i-th step, numerator coefficient vectors $\mathbf{r}_0$ and $\mathbf{r}_1$ can be obtained via least-squares by

$$\underset{\mathbf{r}}{\text{minimize}} \|\mathbf{H}\mathbf{r} - \hat{\mathbf{z}}\|^2, \tag{4}$$

where $\mathbf{r} = [\,\mathbf{r}_0^T\ \mathbf{r}_1^T\,]^T$ is a real-valued vector; $\hat{\mathbf{z}}$ contains K samples of the target frequency response at frequencies $0 \leq \omega_k < \pi$, i.e., $\hat{z}_k = \hat{Z}(\omega_k)$; and $\mathbf{H}$ is a $K \times 2M$ matrix of basis vectors constructed as

$$\mathbf{H} = [\mathbf{h}_{0,1} \cdots \mathbf{h}_{0,m} \cdots \mathbf{h}_{0,M}\, \mathbf{h}_{1,1} \cdots \mathbf{h}_{1,m} \cdots \mathbf{h}_{1,M}\,]$$

with column vectors $\mathbf{h}_{0,m}$ and $\mathbf{h}_{1,m}$ containing the sampled frequency responses of $H_m(z)$ and $z^{-1}H_m(z)$ respectively. With numerator coefficients, we evaluate the frequency response of the model and compute the error measure as the l_2-norm of the difference vector, i.e., $\varepsilon(Z, \hat{Z}) = \|\mathbf{H}\mathbf{r} - \hat{\mathbf{z}}\|^2$.

3.5. Final solution

Once poles have been optimized, numerator coefficients of model (2) are found by solving again problem (4). In Figure 2 we display the frequency response of an example impedance model, obtained from a normalized saxophone impedance measurement after cross-fading to a value of 1 above 8 kHz. Although in principle the model (2) is not guaranteed to be positive-real, fitting to measurements of positive-real functions generally provides positive-real designs. This is important for stability of the sound synthesis model because we need to construct an air column reflectance model that is passive.

4. REALIZATION AS A DIGITAL WAVEGUIDE REFLECTANCE

We treat the air column as a digital impedance load to which we interface the reed model via a pair of decomposed traveling waves. From the input impedance model (2), we construct a reflectance that keeps the state of the air column as a resonating element, and allows us to obtain reflected waves from its interface. Following the digital waveguide formulation for loaded parallel junctions [1], we can compute the scalar flow

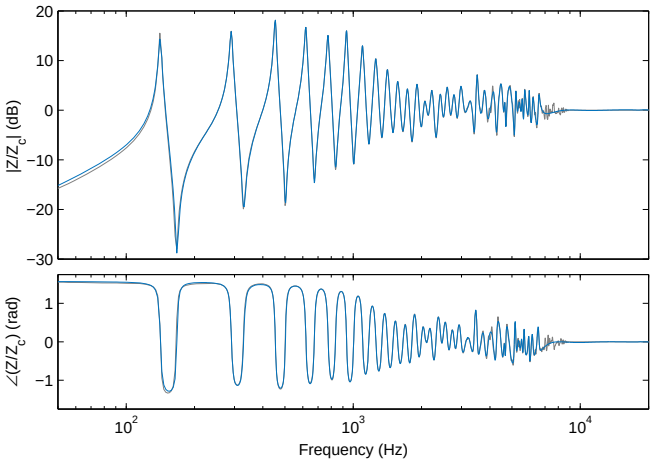

Figure 2. Frequency response of an example saxophone impedance model ('Bb3' fingering), normalized by the characteristic impedance of the input of the air column. Grey and blue curves respectively used for the pre-processed measurement and the model ($M = 35$).

$U(z)$ at the input of the air column solely from the input pressure wave $P^+(z)$ as

$$U(z) = \frac{2Y_c P^+(z)}{1 + Y_c Z(z)} \tag{5}$$

where Y_c is the characteristic admittance of the input of the air column, and $Z(z)$ is the digital impedance model. From the flow $U(z)$, it should be straightforward to compute the scalar pressure $P(z)$ at the input of the air column via

$$P(z) = Z(z)U(z). \tag{6}$$

Finally, from the air column pressure $P(z)$ it is possible to obtain the (reflected) outgoing pressure wave $P^-(z)$ by means of

$$P^-(z) = P(z) - P^+(z). \tag{7}$$

Because the formulation of the impedance model (2) presents a parallel structure that we want to maintain, inverting $Z(z)$ as it appears in equation (5) is impractical. To overcome this problem in the realization of the reflectance, we reformulate the impedance in a similar fashion as we proposed in [4] for the admittance of a string instruments. First, we rewrite each resonator $H_m(z)$ of equation (2) as

$$H_m(z) = 1 + z^{-1} H_m^p(z), \tag{8}$$

with

$$H_m^p(z) = \frac{c_{0,m} + c_{1,m} z^{-1}}{1 + a_{1,m} z^{-1} + a_{2,m} z^{-2}}, \tag{9}$$

$c_{0,m} = -1 - a_{1,m}$, and $c_{1,m} = -a_{2,m}$. Note that denominator coefficients are related to pole radius and angle by $a_{1,m} = -2|p_m|\cos(\angle p_m)$ and $a_{2,m} = |p_m|^2$. We now rewrite the impedance model as

$$Z(z) = B_0 + z^{-1}B_1 + z^{-1}H_0(z) + z^{-2}H_1(z), \tag{10}$$

with

$$B_0 = \sum_{m=1}^{M} c_{0,m}, B_1 = \sum_{m=1}^{M} c_{1,m}, \quad (11)$$

$$H_0(z) = \sum_{m=1}^{M} c_{0,m} H_m^p(z), H_1(z) = \sum_{m=1}^{M} c_{1,m} H_m^p(z). \quad (12)$$

With this new formulation, we rewrite (5) and (6) as

$$U(z) = \frac{2Y_c P^+(z) - z^{-1} Y_c \big(B_1 + H_0(z) + z^{-1} H_1(z)\big) U(z)}{1 + Y_c B_0} \quad (13)$$

and

$$P(z) = B_0 U(z) + z^{-1} \big(B_1 + H_0(z) + z^{-1} H_1(z)\big) U(z). \quad (14)$$

It is important to point out that now the parallel structure appears in the numerator terms $H_0(z)$ and $H_1(z)$, making possible its implementation. Moreover, $H_0(z)$ and $H_1(z)$ can be jointly implemented as a sole bank of parallel resonators. Finally, it is worth mentioning that the term $z^{-1}\big(B_1 + H_0(z) + z^{-1} H_1(z)\big) U(z)$ appears in equations (13) and (14) but does not need to be implemented twice–once it has been computed to obtain $U(z)$ via equation (13), it can be reused to compute $P(z)$ via equation (14).

5. SOUND SYNTHESIS

We construct an efficient sound synthesis scheme by interfacing our air column reflectance model and a modified version of the reed scattering model used in [7] as follows. At each iteration, two main computations are interleaved: the reed scattering update and the air column reflectance update. During the reed scattering update, the differential pressure driving both the reed motion and the reed channel flow relation (see [7]) is first computed as the difference between the mouth pressure and the value of the scalar air column pressure obtained in the previous reflectance update (see Section 4). Then, the pressure wave obtained from the reed scattering is used to feed the next reflectance update. In Figure 3 we display the reed channel flow (see [7]) and the scalar air column pressure P of a synthesis example obtained from an alto saxophone 'Bb3' fingering model, driven by a piecewise linear mouth pressure signal. It can be observed how, during the initial transient, the model first jumps to an upper octave and then transitions to its nominal regime. This model runs about 40 times faster than real-time in one core of a current laptop computer.

6. OUTLOOK

Albeit still preliminary, results shed light on a promising route for efficient, yet realistic sound synthesis with potential applications both in rendering music and in analysing the timbre and playability of real air column prototypes. Among our planned future steps are a more complete exploration with impedances over the full range of notes and of different wind instruments, the development of strategies for transitioning between fingerings, and the modeling of measured radiativities.

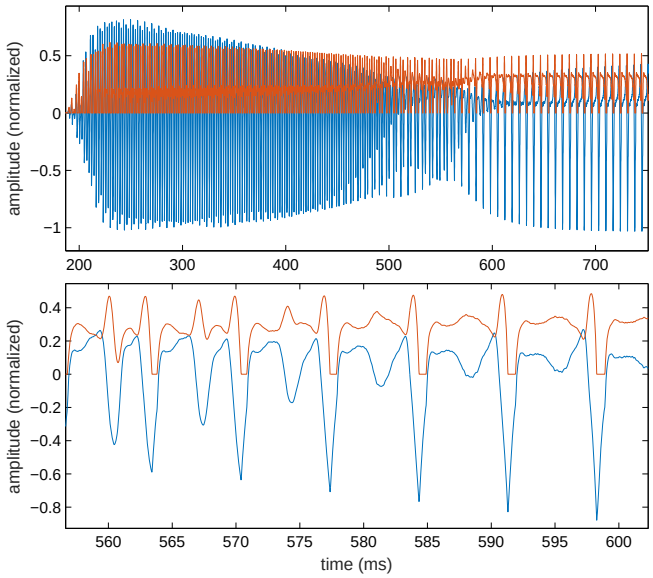

Figure 3. Synthesis example for an alto saxophone 'Bb3' fingering model, driven by a piecewise linear mouth pressure signal. Orange and blue curves respectively used for reed channel flow and air column pressure. Top: initial upper-octave transient. Bottow: detail of the transition towards the nominal regime.

REFERENCES

[1] J. O. Smith, *Physical Audio Signal Processing*. W3K Publishing, 2004. [Online]. Available: http://ccrma.stanford.edu/~jos/pasp/

[2] B. Gazengel, J. Gilbert, and N. Amir, "From the measured input impedance to the synthesis signal: where are the traps?" *Acta Acustica*, vol. 3, pp. 445–472, 1995.

[3] A. Lefevbre and G. P. Scavone, "A comparison of saxophone impedances and their playing behavior," in *Proc. of the Forum Acusticum Conference*, 2011.

[4] E. Maestre, G. P. Scavone, and J. O. Smith, "Digital modeling of bridge driving-point admittances from measurements on violin family instruments," in *Proc. of the Stockholm Music Acoustics Conference*, 2013.

[5] J. Nocedal and S. J. Wright, *Numerical Optimization*. Springer, 2006.

[6] E. Maestre, G. P. Scavone, and J. O. Smith, "Design of recursive digital filters in parallel form by linearly constrained pole optimization," *IEEE Signal Processing Letters*, vol. 23:11, pp. 1547–1550, 2016.

[7] G. P. Scavone and J. O. Smith, "A stable acoustic impedance model of the clarinet using digital waveguides," in *Proc. of the International Conference on Digital Audio Effects*, 2006.